AO10 - Variability of the North Atlantic storm tracks

Supervisors — Drs. S. Osprey and J. Barnett
Candidate no. 46624
Word Count — 3732

Abstract

The frequency with which frontal systems cross the North Atlantic and Europe is determined from UK Meteorological Office synoptic weather charts for 1999 to 2008 using a novel method of analysis. Its variation is investigated as a function of the type of front and season, revealing the mean North Atlantic storm track and maxima of frontal activity near Newfoundland and Iceland, as observed in previous studies, but presenting evidence that the Bergen School model of occlusions is insufficient. The leading order empirical orthogonal function of the data is found to be significantly correlated with the North Atlantic Oscillation, confirming its role in controlling the year-to-year climate variability of western Europe.

1 Introduction

Fronts are thin boundaries between air masses with different thermal characteristics. They are associated with most significant weather events outside of summer as the large thermal gradients present drive assorted air movements and are associated with various types of precipitation (Blumen, 2003).

They were first proposed as part of a model of midlatitude cyclone evolution by the Bergen School in 1919 (Bjerknes, 1919; Bjerknes and Solberg, 1921). This described three types of front associated with cyclones:

- Cold fronts, where cold, dense air moves under warmer, less dense air;
- Warm fronts, a displacement of colder air by warmer air;
- Occluded fronts, described as a cold front overtaking a warm front, such that a region of warmer air is separated from the ground by regions of colder air.

Despite known limitations, reviewed in Mass (1991), this model remains the dominant paradigm for the synoptic analysis of weather systems. This analysis is often summarised on synoptic weather charts, as pictured on the left of figure 1, which are produced daily by regional meteorological bureaus, most often displaying isobars of mean sea level pressure (MSLP) and the locations of fronts, plotted manually by forecasters.

Studies of climate would obviously be interested in any long-term trends in the movement and formation of fronts. However, due to the subjective manner in which they are identified, electronic databases of frontal data are not available.

Previous studies mostly utilised other indicators of weather, such as identifying and tracking cyclones from geopotential height fields (Trigo, 2006) or using bandpass-filtered MSLP charts (extracting variations on the time scale of 2–8 days, corresponding to cyclonic systems) to identify the principal storm tracks as regions of maximum variability (Rogers, 1997; Lau, 1988). Despite using

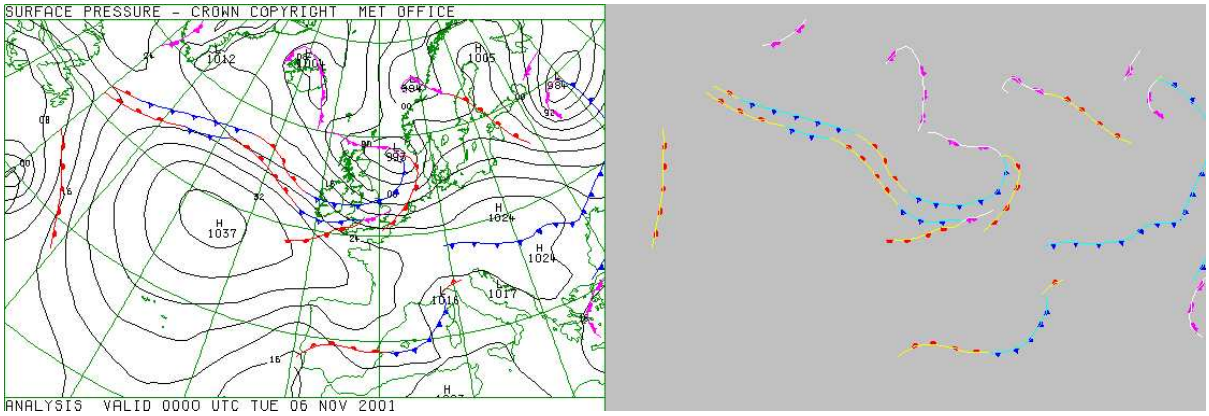

Figure 1: An example of a synoptic chart (left) and the fronts extracted from it (right). The fronts after the removal of labels are plotted as coloured lines (light blue, yellow, white) over the raw fronts (red, blue, pink).

different methods, studies generally find similar basic features (Chang et al., 2002) and so concerns that there may be no proven connection between the features under consideration and actual weather are often overlooked (Reed, 1960).

There are a few examples of studies that directly analyse the variability of fronts. These are time-consuming manual analyses involving counting the number of fronts falling within a pre-defined grid for each chart under consideration (Hardy and Henderson, 2003; Flocas, 1984). These studies only consider the basic features of frontal variability, identifying regions of maximal or minimal frequency and seasonal trends.

The aim of all these studies is to extract information about the primary modes of climate variability. Initially identified by Walker (1924), the North Atlantic Oscillation (NAO) is considered the primary mode of climate variability in the Atlantic basin outside of summer (Wanner et al., 2001). It is represented by variations in pressure between regions near the Azores and Iceland, such that when pressures are anomalously high in the subtropics, they are anomalously low near Iceland and vice versa. As reviewed in Marshall et al. (2001), the NAO determines the magnitude of the meridional pressure gradient over the North Atlantic and, thus, the strength and direction of geostrophic winds across the region.

Walker and Bliss (1932) proposed an index to characterise the state of the NAO — the normalised, time-averaged pressure difference between two monitoring stations near the centres of action, most often Iceland and the Azores (or Portugal). Broadly, a positive NAO index corresponds to higher than usual pressures in the mid-Atlantic, which produces stronger westerlies, directs storm tracks more towards Scandinavia (Hurrel and van Loon, 1997, sec. 3(d)), and results in warmer, drier winters across central and southern Europe (Hurrel, 1995).

2 Data and Methodology

This study analysed daily synoptic weather charts from June 1999 to December 2008 (UK Meteorological Office, 2009). These GIF images display MSLP fields and fronts daily at 0000 UTC for 50°W–45°E, 35°N–75°N. By manual inspection, a small number of flawed

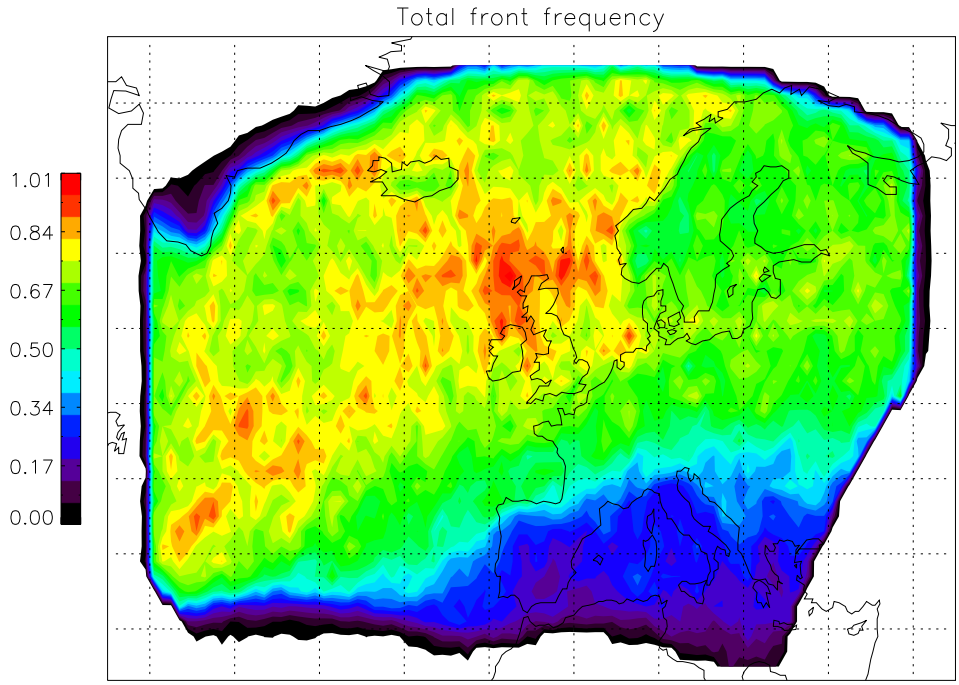

Figure 2: Spatial variation in frontal frequency for 1999–2008 (fronts per day per 100km^2). Note that white represents both 'no data' and a frequency of exactly zero.

charts were removed. Occasionally, multiple charts were produced for a single day due to rapidly changing forecasts, in which case the chart with the earliest time stamp was accepted.

This image format simplifies computer analysis as the fronts are plotted in colour, indicated by an integer index at each point on a uniform grid. From this, algorithms developed for this work (described in the appendix) can efficiently extract the pixels corresponding to a given type of front.

As presented on the charts, the fronts included labels (triangles for a cold front, etc.) indistinguishable from the fronts to the algorithms. These were removed by noting that the fronts were drawn as lines one pixel wide. Thus, any pixel identified as representing a front, but having more than two neighbouring pixels also identified as representing fronts, must be within a label and so are ignored. Interpolation was then used to join the resulting line segments to form 'clean' fronts, as shown in figure 1. (For a full description, see the appendix.)

Charts summarising the frequency with which frontal systems crossed each pixel (such as figure 2) were produced by 'adding' together the daily charts within a given period and dividing by the number of days in that period. Front frequency was considered as it allows averages over periods of different durations, due to missing data, for example, to be compared objectively.

The original weather charts were plotted on a polar stereographic projection, for which the surface area covered by a pixel varies across the image. To objectively compare front density at different latitudes, the frequency of a pixel was weighted by dividing by the surface area

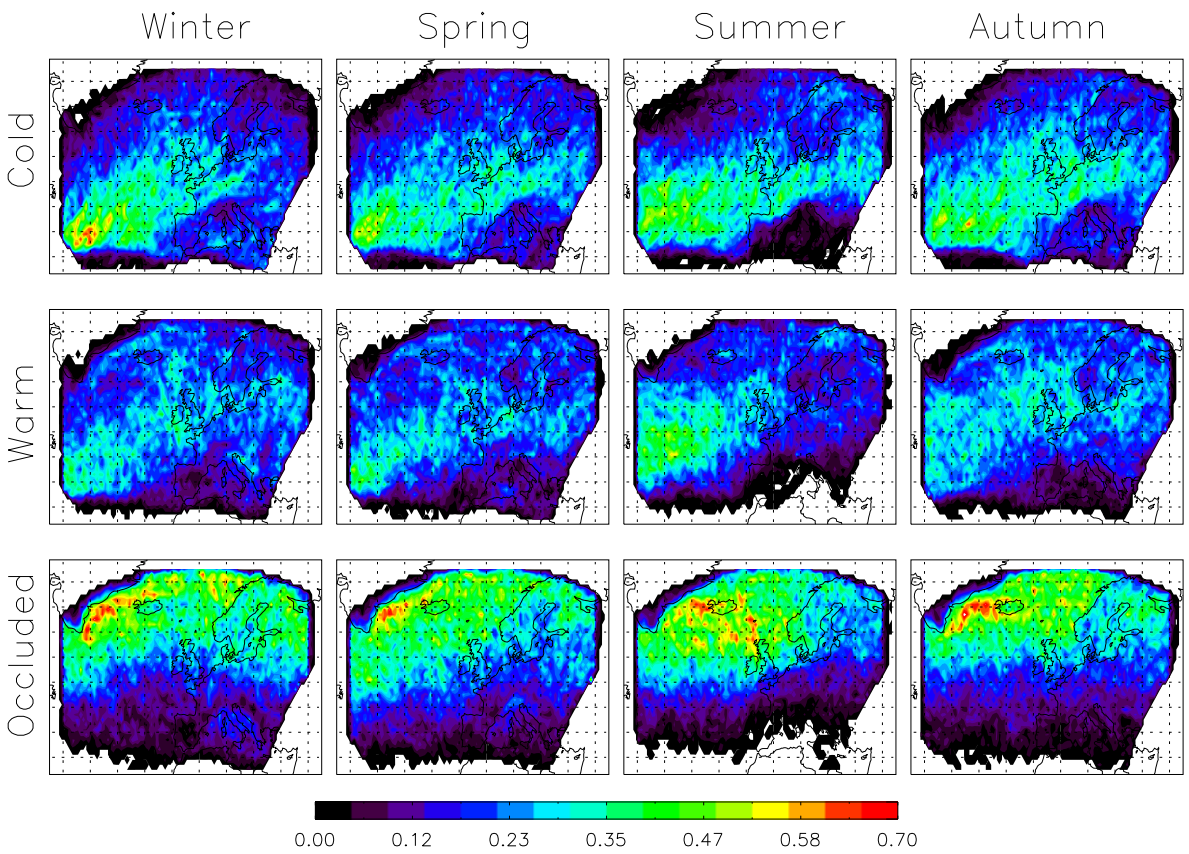

Figure 3: As figure 2, but divided into components by season and type of front.

covered by that pixel.

The latitude, θ, and longitude, ϕ, for the vertices of each pixel are determined by the polar stereographic inverse transformations,

$$\theta = \frac{\pi}{2} - \arctan\frac{\sqrt{x^2+y^2}}{R_\oplus}; \qquad \phi = \arctan\frac{x}{y},$$

where x and y are coordinates in the image plane relative to the North Pole and $R_\oplus$ is the diameter of the Earth in the units of the image.

From these coordinates, the "great circle" distance along a given edge, $aR_\oplus$, is determined using the spherical equivalent of the Pythagorean theorem,

$$\cos a = \cos\Delta\theta\cos\Delta\phi, \tag{1}$$

where $\Delta\theta\,(\Delta\phi)$ is the difference between the latitudes (longitudes) of the vertices of that edge.

A square pixel in the image corresponds to an irregular spherical quadrilateral on the surface of the Earth. To determine its area, one divides it into two spherical triangles. The area of one of them, with side 'lengths' a, b, c determined from equation 1 is,

$$A = 4R_\oplus^2 \arctan\sqrt{B}, \tag{2}$$

where $B = \tan\frac{a+b+c}{4}\tan\frac{b+c}{4}\tan\frac{a+c}{4}\tan\frac{a+b}{4}$, as outlined in Miller (1994).

To reduce noise, the data was re-sampled onto a coarser, isotropic latitude-longitude grid (inspired by Flocas (1984)) by taking the average value of all pixels that fall within each

new grid square. A $1° \times 1°$ grid was selected as it provided a reasonable contrast between background noise and maxima.

The leading empirical orthogonal functions (EOFs) were then calculated to provide some indication of the primary modes of variability of the system. EOF analysis is an eigenfunction analysis technique similar to Fourier analysis, but rather than decomposing the data over given base functions, the base functions are determined from the data to 'explain' the maximum possible variance. The procedure returns n orthogonal functions, $\mathrm{F}_n(\mathbf{r})$, each with a corresponding time series (known as principal components (PCs)), $\mathrm{p}_n(t)$, from which the original data can be expressed as,

$$\mathrm{f}(\mathbf{r}, t) = \sum_{i=1}^{n} \mathrm{p}_n(t)\mathrm{F}_n(\mathbf{r}).$$

(Full details can be found in Hallor and Venegas (1997).)

It is necessary to remove known variations from the data before such an analysis is performed; otherwise they will dominate the results. The data was de-seasonalized by subtracting a climatological mean[1] from each monthly chart. A possible linear trend in the monthly mean frequency was removed by subtracting a least-squares fit trend point[2] from each value within each chart. The data was truncated before January 2002 such that each month is equally represented in the data. The month of February 2003 was later removed from the data as it exhibited an anomalously large variance.

[1] All charts for a given month were added together and divided by the number of months used.

[2] A monthly mean frequency was determined by summing across all data points in that chart and dividing by the number of points. A linear trend was then fitted to the variation in this mean over time.

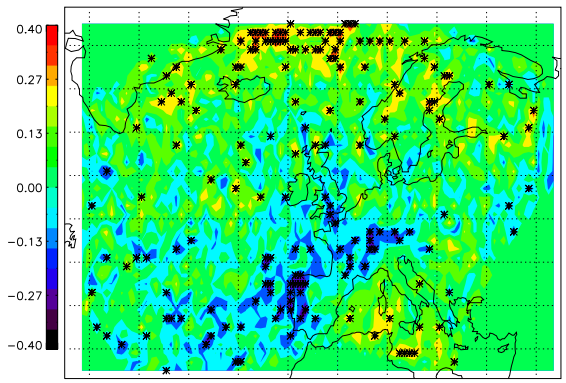

Figure 4: Distribution of correlation between total front frequency and the NAO index for Jul 2001 – Dec 2008. Statistically significant points (from a two-tailed t-test at the 5% confidence level) are highlighted with an asterisk.

3 Results and Discussion

3.1 General distribution

The variation in frequency for all types of front across the entire data set is shown in figure 2 (in general agreement with fig. 2 of Schumann and van Rooy (1951) and fig. 3 of de la Torre et al. (2008)). One observes that frequencies over land are generally lower than over sea. This is expected as land has a lower effective heat capacity than sea, so the thermal contrast between them is smaller than between sea and air. The reduction in energy available to the fronts causes them to dissipate.

The effects of mountainous regions on fronts is still a topic of debate (summarised in Egger and Hoinka (1992)), but this data clearly shows that fronts avoid the coast of Greenland. There are also marked decreases in frequency south of the Alps and at the Norwegian coast, indicating mountainous regions encourage the dissipation of fronts.

There are weak indications of the Mediterranean maxima found in Trigo (2006) and Reed

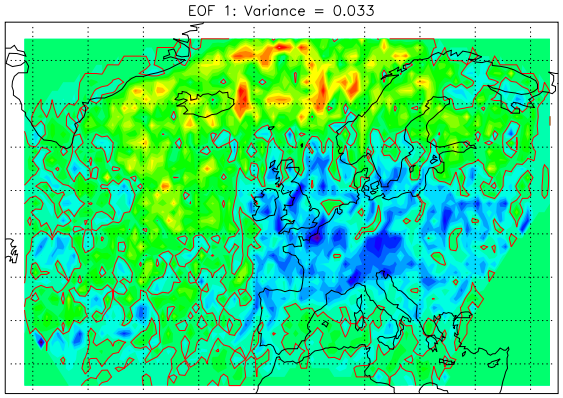

Figure 5: The leading order EOF of monthly mean frequency deviation (zero contour plotted in red). This explains 3.3% of the total variance of the data.

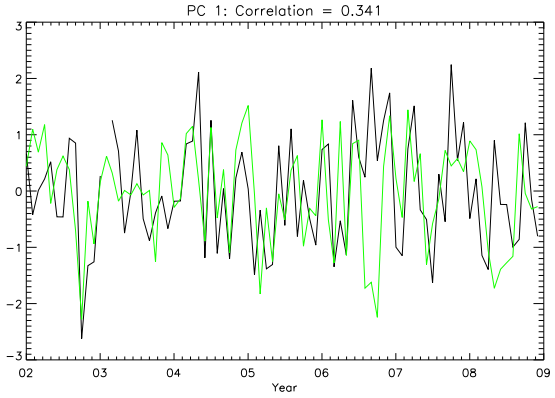

Figure 6: The principal component for figure 5 (black) and the NAO index (green). The correlation between them is 0.341, which is significant at the 1% level, with 87 degrees of freedom. Note that February 2003 has been removed.

(1960) along the Croatian coast and near Sardinia. The lack of prominence of this feature in the data is possibly due to its position near the southern limit of the data region. Forecasters may have considered this region to be of lesser interest and neglected it on some occasions.

Previous studies have associated areas of increased baroclinicity[3] or enhanced orography with frontogenesis and storm tracks, particularly the areas east of Newfoundland (Rogers, 1997; Lau, 1988) and near the Denmark Strait (Trigo, 2006, figs. 1 and 2). These regions are investigated in figure 3 by considering the seasonal and categorical components of the general distribution. One observes that these areas exhibit maxima in the frequency of cold and occluded fronts, respectively. It is interesting to note that the prominent maxima off Scotland in figure 2 is only observed in the summer occluded chart, and was not observed in previous studies, suggesting it is more of a statistical effect than an actual feature.

In the Bergen School model of fronts, occluded fronts are produced when a cold front overlaps a warm front. If this were the case, we would expect a maxima for occluded fronts to occur where cold and warm fronts coincide. In this data, the maxima actually occurs in a region of relatively little cold and warm front activity. This supports the arguments of Mass (1991) that the Bergen School model needs to be updated to represent the fronts actually produced by forecasters.

Also, the Denmark Strait has previously been specifically associated with cyclogenesis (de la Torre et al., 2008), but is observed here to be a region of occluded front activity. This suggests occluded frontogenesis has occurred, a process currently poorly explained as it is not included within the Bergen School model.

The mean Atlantic storm track is evident in the cold and warm front signals as bands of increased frequency leading from the North American coast to Great Britain (Lau, 1988, fig. 1 for comparison). This is expected as the storm track represents the primary regions of cyclone activity, which is very closely related

[3] A measure of the stratification of the atmosphere, baroclinicity is generally associated with the genesis of highs and lows.

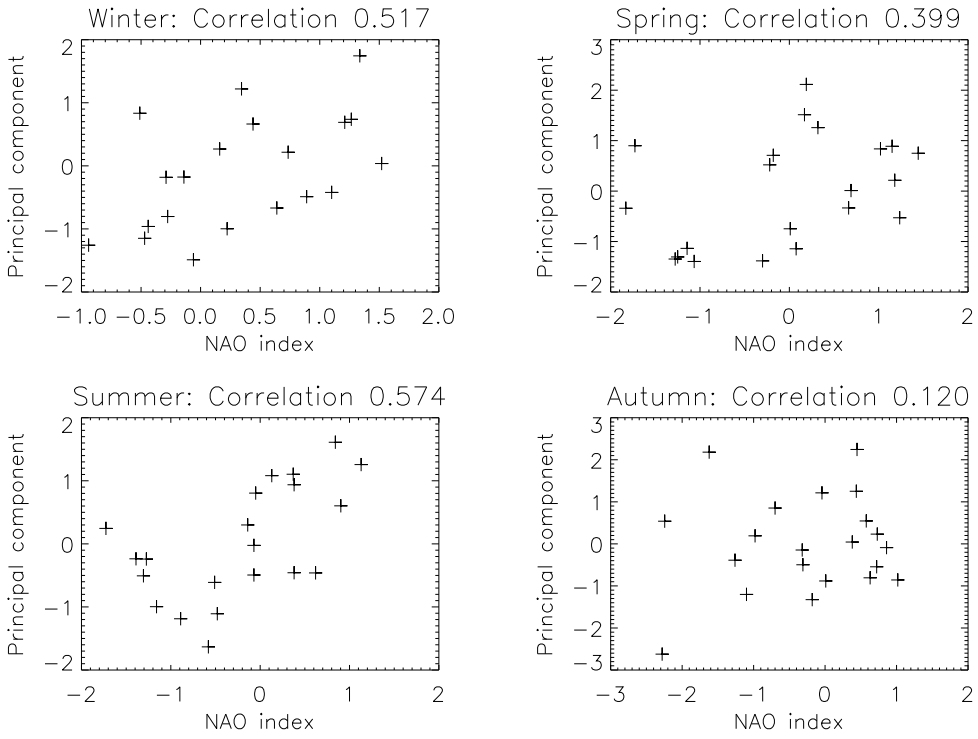

Figure 7: Scatter plots of the amplitude of the first PC against NAO index for each season of the year, listing their respective correlations. At the 5% level, winter and summer present significant correlations, using 19 degrees of freedom (18 for winter).

to frontal activity. The track is dominated by cold fronts during winter and by both cold and warm fronts during summer. One also observes the relative weakness of warm fronts compared to cold fronts (described in Hines and Mechoso (1993)), as they exhibit lower frequencies than cold fronts within this track and show more pronounced attenuation over land.

3.2 Influence of the North Atlantic Oscillation

As a first consideration, figure 4 was produced. It shows the point-wise correlation between monthly front frequency and the NAO index (derived by the National Weather Service (2009)). The longest continuous period of monthly data available, July 2001 to December 2008, was used. The results present a dipole structure similar to the leading pattern of the NAO, concentrated in regions near Iceland and Portugal, and indicate that, as expected, when the NAO index is positive, frontal systems pass more frequently over the Norwegian Sea and less frequently over continental Europe.

Shown in figures 5 and 6, the leading order EOF for the data presents a similar spatial pattern to the NAO. Its correlation with the NAO index is significant at the 1% confidence level. This suggests that the leading order function represents the forcing of the NAO on fronts and that this is a dominant forcing. The general form of this function was found to be independent of the grid size used for resampling (i.e. when using a $5° \times 5°$ grid rather

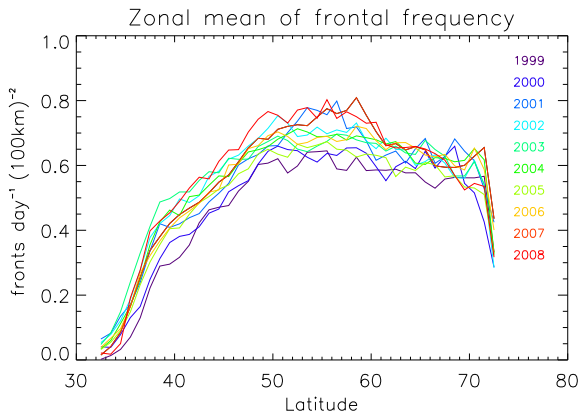

Figure 8: Variation in the zonal mean of front frequency with latitude by year.

than a $1° \times 1°$ grid), unlike lower order functions, suggesting it represents a physical signal. The low percentage of variance explained by the mode is likely due to substantial noise produced by the sparseness of the frontal data.

To further investigate this forcing, figure 7 shows the seasonal components of the relation between the NAO index and the amplitude of the first PC. The NAO, though present thoughout the year, is generally considered dominant in the winter (Rogers, 1990, table 1). This is substantiated by the significant correlation observed in winter. However, the correlation seen in summer is unexpected and should be further analysed in future work.

The consistency of the data was further investigated by considering the variation in the zonal mean of front frequency over time (without de-seasonalizing or de-trending the data). Shown in figure 8, each year exhibits the same general pattern and there is no evident yearly trend, indicating that consistent methods were applied by forecasters in the data's production over time (though this does not eliminate the possibility of a bias independent of latitude).

4 Conclusions

The daily distributions of fronts over the North Atlantic and Europe were extracted from UKMO synoptic charts and the spatial and temporal variability of these analysed over the period 1999–2008. The spatial distribution (fig. 2) was found to be in agreement with previous studies of cyclone activity in the region. Maxima in frequency were observed off the coast of Newfoundland and over the Denmark Strait, regions associated with increased baroclinicity at the land-sea boundary.

Advancing on previous work, these maxima were specifically associated with cold and occluded fronts, respectively. In particular, it was observed that cold and warm fronts do not generally intersect areas occupied by occluded fronts (fig. 3). This does not support the often quoted model that occluded fronts occur when a cold front overlaps a warm front (for example, in Schultz (1996)), which would imply an intersection of the three types of front. This work supports the conclusions of Mass (1991) that a more appropriate conceptual model should be produced to describe fronts that represents the physical processes actually observed (such as occluded cyclogenesis) and the fronts produced by forecasters.

The association of the NAO with the front frequency distribution was investigated. After removing expected seasonal and annual trends, it was found that the leading order EOF of the data is correlated with the NAO index, significant at the 1% level according to a two-tailed t-test. It presents a pattern consistent with the NAO paradigm — during times associated with a positive NAO index, more fronts are directed towards Scandinavia and fewer towards continental Europe. This driving was most pronounced, as expected, in winter and, surprisingly, in summer. Further investigation of these results would be worthwhile, such as considering the possibility of autocorrelation

within the data.

A possibility for future work is suggested by the methods of Hewson (1998). Currently available gridded data sets of atmospheric tracers, such as potential temperature, can be used to objectively determine the positions and trajectories of fronts. This removes the possibility of bias being introduced by forecasters and vastly increases the range of time and space that can be considered. Such methods were used successfully in the recently published work of de la Torre et al. (2008).

Overall, the fact that this relatively simple analysis of synoptic weather charts across only a few years has found reasonable evidence linking the NAO with the climate of the North Atlantic further demonstrates that the NAO is a true physical mode of the Earth's climate and not just a statistical convenience.

Acknowledgements I would like to thank my supervisors for all their preliminary work (especially the coordinate transformations), advice, and support. This project could not have been completed without their tireless assistance. This work would not have been possible without the data kindly provided by the BADC and UK Met Office. I also wish to thank Drs. W. Ingram and T. Hewson for some very inspirational conversations on current forecasting methods. Finally, thanks to Rhys and Mom for their proof-reading.

Appendix: The front extraction algorithm

The primary difference between this study and previous work is its use of digital front information, as extracted from synoptic weather charts. This was facilitated by the charts being stored as 8-bit GIF images. Reading such an image with the IDL function `read_gif` returns (after removing a section containing a forecast not considered in this study) a 560×380 integer array, where the value at each point represents its colour. Relevant colours were blue, red, and pink which are represented by indices of 1, 2, and 3 respectively. The locations of pixels representing fronts could thus be extracted using code such as,

```
where(image eq 1),
```

where `image` is the integer array.

The triangular or semicircular labels on these fronts then needed to be removed as the number of pixels within such labels is of a similar order to the number actually representing fronts and would swamp any possible signal. The methods available were greatly limited by the inconsistent rendering of these labels. Their exact size, the distance between labels, and their position along the front vary greatly and the labels are not always uniformly filled. The algorithm developed utilises the fact that the fronts, as drawn, are only one pixel wide and so any pixel identified as representing a front, but having more than two neighbours also identified as representing fronts, must be within a label. It then ignores these points and interpolates a new line to connect the remaining line segments.

In summary, using the term 'point' to mean a pixel identified as representing a given type of front:

1. Use `label_region` to mark all points within each front with a number, such that if two points are marked with the same number, they can be joined by a series of adjacent of points with an identical mark;
2. For each point, calculate the number of points adjacent to it ('neighbours');
3. Identify all points with more than two neighbours and flag them as points within a label;
4. In order to remove points at the edge of a label, such as the tip of a triangle, find all

currently unflagged points that are not adjacent to any other unflagged points. Flag these points as within a label;

5. Identify all points that have not been flagged, but which neighbour a point that has been. Flag these points as the edges of labels;

6. Remove all points flagged as being within a label from the data, leaving a series of line segments;

7. Use `label_region` again to mark these line segments with a second number;

8. Consider a point flagged as the edge of a label. Determine the nearest other point that is marked as being on the same front (from 1) but is not on the same line segment (from 7). A maximum distance is included such that if a label crosses the edge of the image, its single edge will not be further processed;

9. Draw a line between these two points;

10. Repeat 8 and 9 until all edges are joined.

This method fairly accurately extracts the fronts (fig. 1). The line drawn does not solely correspond to points determined to be fronts, but the presence of empty spaces in the labels prohibited such a check. If a front ends with a label, the front is truncated at the last edge. It avoids joining points not on the same front and joining two points that are already connected by a front.

However, if two different fronts physically touch somewhere, the algorithm will join points not on the same front. From the manual scan of the raw data, it is believed this only occurs a few times, and so the effects are negligible.

References

Bjerknes, J., 1919: On the structure of moving cylones. *Geofysisk Publikationer*, **1**, 1–8.

Bjerknes, J. and H. Solberg, 1921: Meteorological conditions for the formation for rain. *Geofysisk Publikationer*, **2**, 1–60.

Blumen, W., 2003: *Fronts*, 805–813. Encyclopedia of Atmospheric Sciences, Academic Press, San Diego, CA.

Chang, E., S. Lee, and K. Swanson, 2002: Storm track dynamics. *Journal of Climate*, **15 (16)**, 2163–2183.

de la Torre, L., R. Nieto, M. Nogruerol, J. A. Anel, and L. Gimeno, 2008: A Climatology Based on Reanalysis of Baroclinic Developmental Regions in the Extratropical Northern Hemisphere. *Trends and Directions in Climate Research*, Gimeno, L and Garcia-Herrera, R and Trigo, RM, Ed., Annals of the New York Academy of Sciences, Vol. 1146, 235–255, 7th European-Meteorolog-Society Annual Meeting.

Egger, J. and K. Hoinka, 1992: Fronts and orography. *Meteorology and Atmospheric Physics*, **48 (1-4)**, 3–36.

Flocas, A., 1984: The annual and seasonal distribution of fronts over central-southern Europe and the Mediterranean. *Journal of Climatology*, **4 (3)**, 255–267.

Hallor, B. and S. Venegas, 1997: *A manual for EOF and SVD analyses of climate data*. Available at `http://andvari.vedur.is/~halldor/TEXT/eofsvd.html`.

Hardy, J. and K. Henderson, 2003: Cold front variability in the southern United States and the influence of atmospheric teleconnection patterns. *Physical Geography*, **24 (2)**, 120–137.

Hewson, T., 1998: Objective fronts. *Meteorological Applications*, **5**, 37–65.

Hines, K. and C. Mechoso, 1993: Influence of surface drag on the evolution of fronts. *Monthly Weather Review*, **121 (4)**, 1152–1175.

Hurrel, J., 1995: Decadal trends in the North-Atlantic Oscillation – regional temperatures and precipitation. *Science*, **269 (5224)**, 676–679.

Hurrel, J. and H. van Loon, 1997: Decadal variations in climate associated with the North Atlantic Oscillation. *Climatic Change*, **36**, 301–326.

Lau, N., 1988: Variability of the observed midlatitude storm tracks in relation to low-frequency changes in the circulation pattern. *Journal of the Atmospheric Sciences*, **45 (19)**, 2718–2743.

Lowry, R., 2009: *Concepts and Applications of Inferential Statistics*. Vassar College, Poughkeepsie, NY, available at `http://faculty.vassar.edu/lowry/webtext.html`. (Provided sampling distributions of t-test.).

Marshall, J., et al., 2001: North Atlantic climate variability: Phenomena, impacts and mechanisms. *International Journal of Climatology*, **21 (15)**, 1863–1898.

Mass, C., 1991: Synoptic frontal analysis - time for a reassessment. *Bulletin of the American Meteorological Society*, **72 (3)**, 348–363.

Miller, R., 1994: *Computing the area of a spherical polygon*, 132–137. Graphic Gems IV, Academic Press, San Diego, CA.

National Weather Service, 2009: *Monthly mean NAO index, [Internet]*. Available at `www.cpc.ncep.noaa.gov/products/precip/CWlink/pna/nao.shtml`. (Rather than a station-based index, this represents the interpolation of the loading pattern of the NAO onto daily 500-mb anomalies.).

Reed, R., 1960: Principal frontal zones of the Northern Hempishpere in winter and summer. *Bulletein of the American Meteorological Society*, **41**, 591.

Rogers, J., 1990: Patterns of low-frequency monthly sea-level pressure variability (1899-1986) and associated wave cyclone frequencies. *Journal of Climate*, **3 (12)**, 1364–1379.

Rogers, J., 1997: North Atlantic storm track variability and its association to the north Atlantic oscillation and climate variability of northern Europe. *Journal of Climate*, **10 (7)**, 1635–1647.

Schultz, D., 1996: *Occluded fronts*, 544–546. Encyclopedia of Climate and Weather, Oxford University Press.

Schumann, T. and M. van Rooy, 1951: Frequency of fronts in the Northern Hemisphere. *Meteorology and Atmospheric Physics*, **4**, 87–97.

Trigo, I., 2006: Climatology and interannual variability of storm-tracks in the Euro-Atlantic sector: a comparison between ERA-40 and NCEP/NCAR reanalyses. *Climate Dynamics*, **26 (2-3)**, 127–143.

UK Meteorological Office, 2009: *Mean Sea Level Pressure charts, [Internet]*. British Atmospheric Data Centre, available at `http://badc.nerc.ac.uk/data/ukmo-charts`.

Walker, G., 1924: Correlations in seasonal variations of weather IX. *Memoirs India: Meteorological Department*, **24**, 687–692.

Walker, G. and E. Bliss, 1932: World Weather V. *Memoirs of the Royal Meteorological Society*, **4**, 53–84.

Wanner, H., S. Bronnimann, C. Casty, D. Gyalistras, J. Luterbacher, C. Schmutz, D. Stephenson, and E. Xoplaki, 2001: North Atlantic Oscillation - Concepts and studies. *Surveys in Geophysics*, **22 (4)**, 321–382.